Temperature and Strain Rate Independence of Critical Strains in Polyethylene and Poly(ethylene-*co*-vinyl acetate)

S. Hobeika, Y. Men, and G. Strobl*

Fakultät für Physik der, Albert-Ludwigs-Universität, 79104 Freiburg, Federal Republic of Germany

Received June 29, 1999; Revised Manuscript Received November 29, 1999

ABSTRACT: True stress−strain curves measured during uniaxial tensile deformations of polyethylene generally show four characteristic points where the differential compliance and the recovery properties change. They can be associated with the onset of isolated inter- and intralamellar slip processes (point A), a change into a collective activity of slips (B), the beginning of crystallite fragmentation (C), and chain disentanglement (D). Experiments were carried out for high density polyethylene, low density polyethylene, and an ethylene−vinyl acetate copolymer, with variation of the temperature and the strain rate. While the stresses at the critical points change remarkably, the related strains turn out as constant. The only exception is point D, which shifts to lower strains on heating. Observations correspond with the previously found independence of the critical strains on the crystallinity.

1. Introduction

Deformation of semicrystalline polymers is always accompanied by changes in the microscopic structure that result in an alteration of sample properties during deformation. In a recent study (Hiss;[1] the paper provides also a survey of previous works), we investigated the effect of crystallinity on the mechanical, elastic, and structural behavior of polyethylene and related copolymers by means of video-controlled uniaxial drawing with constant strain rate, step-cycle tensile tests analyzing the elastic recovery, and wide-angle X-ray scattering experiments for texture determinations under load. It was found that despite the large variations in the global mechanical properties from solidlike to rubber-like the deformation behavior follows a common general scheme. There exist four transition points, denoted A, B, C, and D, where the differential compliance, the reversibility of the imposed strain, and the crystallite texture change simultaneously. These points may be associated with

1. the onset of isolated inter- and intralamellar slip processes (point A),
2. a change into a collective activity of slips (point B),
3. the beginning of fibril formation after a fragmentation of the lamellar crystals (point C), and
4. chain disentanglement (point D).

While the stresses at these points greatly vary with crystallinity, the strains remain essentially constant. Crystal textures are found to be a function of the imposed strain only, the dependencies being common for all samples. Obviously, crystallites are able to easily react to the imposed deformation in a well-defined manner, determined only by the strain. This suggests that coarse block-slip processes are generally activated, for linear polyethylene and the copolymers likewise, thus providing sufficient degrees of freedom for accomplishing any deformation. In fact, recent studies of various crystallizing polymers by time-dependent SAXS and AFM[2,3] have shown that the building-up of the lamellae is always a two-step process, beginning with the formation of blocks which then fuse into layers. As a memory of this building process, lamellae retain a granular substructure.

An obvious question arising from the work was, if crystallinity does not change these critical strains, does a variation of temperature and strain rate have any effect? We therefore continued our studies by varying these parameters. As is described in the following sections, we found that the critical states of deformation are independent of these parameters.

2. Experimental Section

2.1. Materials. For the analysis of the temperature and strain rate dependence of the yielding properties, we selected three samples with quite different crystallinities: a linear polyethylene (Hoechst AG, Frankfurt) with 76% crystallinity (HDPE), a branched polyethylene (BASF AG, Ludwigshafen) with 46% crystallinity (LDPE33), and a polyethylene−vinyl acetate copolymer (Exxon Chemical Europe, Machelen, Belgium) with a crystallinity of 26% (PEVA18). Their properties and the sample preparation were described in a previous paper.[1]

2.2. Small-Angle X-ray Scattering and Differential Scanning Calorimetry. To study the temperature dependence of a polymer's mechanical properties, it is important to know the effect that heating has on morphology. Differential scanning calorimetry (DSC) is a suitable method for determining the temperature-dependent crystallinity, which follows at each temperature from the remaining heat of fusion. Small-angle X-ray scattering (SAXS) gives information about changes in lamellar structure during heating. DSC and SAXS specimens and the "dog bone" specimens for the tensile tests were cut from the same melt pressed sheets.

DSC experiments were performed in a Perkin-Elmer DSC-4 at a heating rate of 10 K/min. SAXS experiments were carried out using a conventional X-ray Cu Kα tube and a Kratky compact camera combined with a sample holder with heating facilities and a temperature control. Scattering data were analyzed in the usual way, by calculating the one-dimensional electron density autocorrelation function and deducing the thicknesses of crystalline and amorphous layers as well as the linear crystallinity (compare Strobl,[4] p 408).

* To whom correspondence should be addressed.

10.1021/ma9910484 CCC: $19.00
Published on Web 02/12/2000

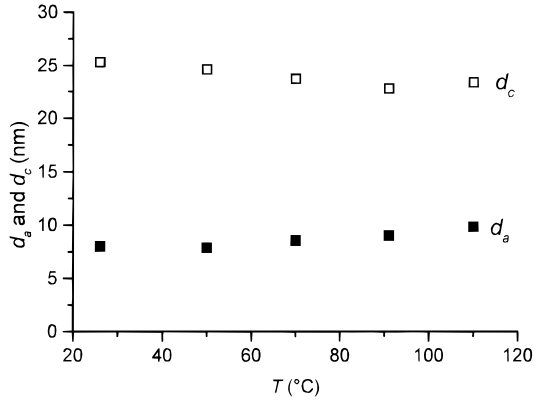

Figure 1. Temperature dependence of the thickness of the crystalline lamella d_c (*open symbols*) and of the amorphous layer d_a (*filled symbols*) for the HDPE sample, taken from a SAXS experiment.

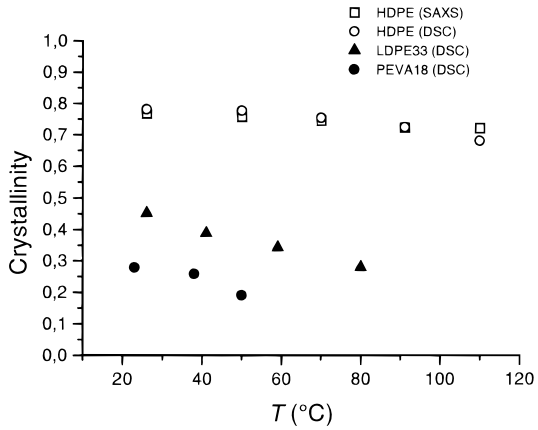

Figure 2. Temperature dependence of the crystallinity derived from SAXS curves for HDPE and from DSC data for all samples.

2.3. Mechanical Testing. True stress−strain curves were measured using an INSTRON 4301 machine equipped with a video control that maintained a constant local strain rate in the narrowest part of the specimen, as first used by G'Sell.[5] Elastic properties in the deformed state were derived from step-cycle tests, which combine stepwise stretching of the samples with unloading-reloading cycles, and from determinations of the free shrinkage after unloading, observed at the measuring temperature and also during heating to the melting peak. All experimental details have already been given.[1] The temperature was controlled using an INSTRON 3111 heating chamber with a range from room temperature up to 200 °C.

3. Results

3.1. Analysis of Partial Melting by SAXS and DSC. Figure 1 gives the results of the temperature-dependent SAXS experiments for HDPE. Observations are indicative for a reversible surface melting (compare Strobl,[4] chapter 4.3) as the thickness d_a of the amorphous layers increases and the thickness of the crystalline lamellae correspondingly decreases on heating (at 110 °C, the surface melting is superposed by an irreversible crystal thickening). The DSC melting curves of LDPE33 and PEVA18 indicate that the secondary crystallization during cooling here produced lamellae with a wide range of thicknesses which, during heating, then melt in reverse order.

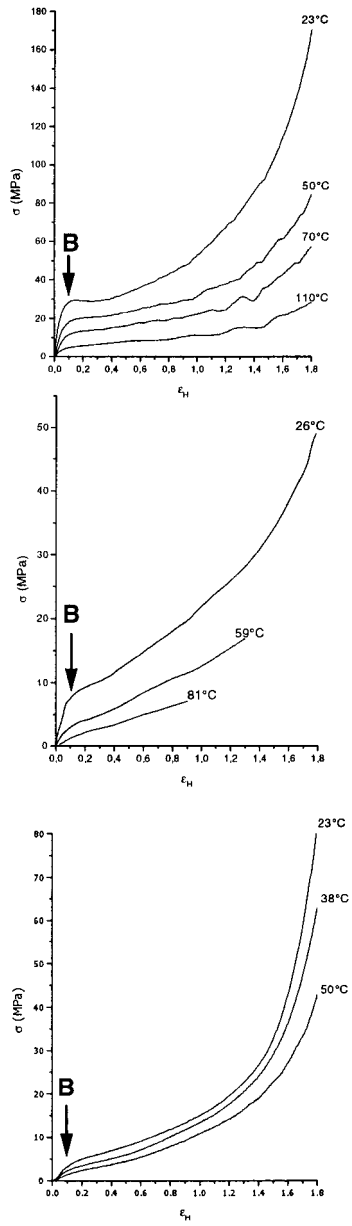

Figure 3. True stress−strain curves, measured at a constant Hencky strain rate of 5×10^{-3} s^{-1} at the temperatures indicated in the plot for HDPE (*top*), LDPE33 (*center*), and PEVA18 (*bottom*).

Figure 2 shows the temperature dependence of the crystallinity for the three samples in the range of the mechanical tests. SAXS and DSC give equal results for HDPE, both indicating that changes in crystallinity caused by the surface melting are much smaller than those resulting from the melting of the inserted lamellae in LDPE33 and PEVA18. We thus get two different temperature dependencies of the morphology of the two samples: a change in the number of crystallites on heating in the case of LDPE33 and PEVA18 on one hand and no influence of temperature on this number for the HDPE sample on the other hand.

3.2. Effect of Temperature on Deformation Behavior. True stress−strain curves for all samples measured at different temperatures are shown in Figure 3. Increasing the temperature leads to a general reduction of the applied stress. As shown in the previous work, from the stress−strain curves the transition point B, which comes near to the yield point observed in

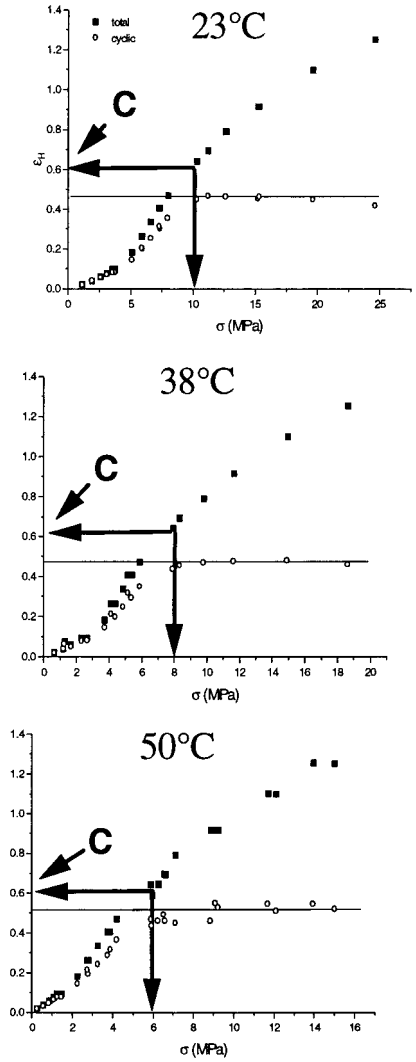

Figure 4. Total strain and cyclic strain component as a function of imposed stress, derived for PEVA18 from step-cycle tests under variation of the temperature.

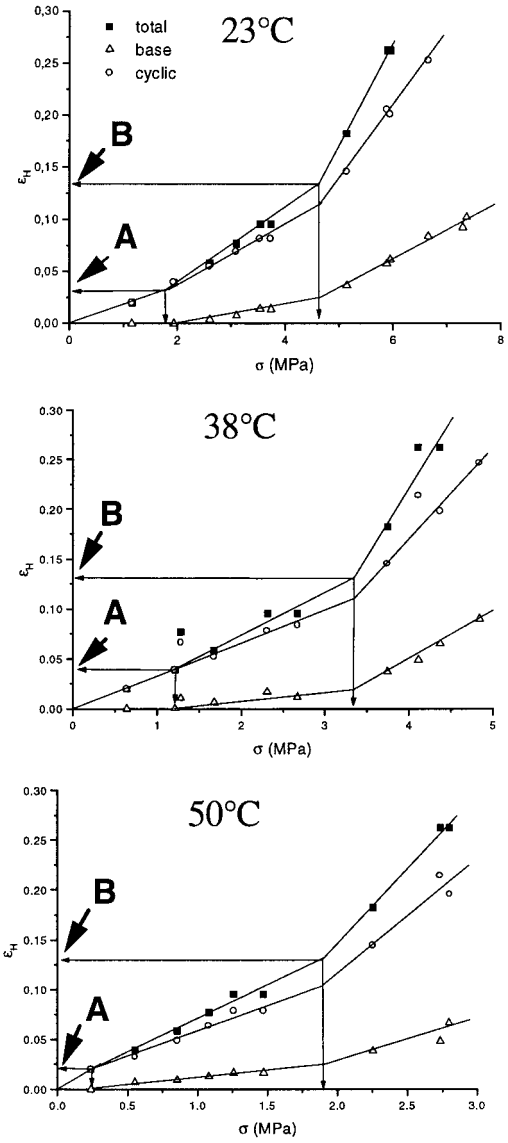

Figure 5. PEVA18 at different temperatures: partitioning of the total strain into the cyclic and the base component for small strain values (enlarged view from Figure 4).

engineering tensile tests, can be determined. It is located in the range with the largest changes in the differential compliance, that is, the maximum curvature of the stress−strain curve. It can clearly be seen that although the stresses at the yield points remarkably decrease with temperature, the yield strains essentially remain constant at $\epsilon_H \approx 0.12$.

At all four transition points, characteristic changes take place in the elastic recovery properties of the samples. As previously, the recovery of the imposed deformation was investigated by performing step-cycle tests, now with the focus on the effect of temperature. Step-cycle tests give a partitioning of a total imposed strain into two components, a spontaneously reversible "cyclic part" and a "base part" that is irreversible on the time-scale of this experiment. Figure 4 shows the changes with temperature of the total strain and the recoverable cyclic component, as obtained for PEVA18 as a function of the applied stress. The clearest change in elastic behavior is given by the cyclic component reaching a plateau. This marks the transition point C, where, as shown in the previous work, fibrillation sets in. Note that although the stresses at point C decrease with increasing temperature, the related total strain remains constant at $\epsilon_H \approx 0.6$.

A closer look at the low-deformation region (Figure 5) shows the same temperature independence for the two other transition points A and B. At A, associated with the onset of individual slip processes, for the first time irreversible strains $\epsilon_{H,b}$ arise. Then, at point B, a strong increase in the differential compliance is observed. It is caused by increases of both the recoverable and the permanent part. For all temperatures, we find point A at a strain $\epsilon_H \approx 0.03$ and point B at $\epsilon_H \approx 0.13$.

Figures 6 and 7 show data from analogous experiments carried out for LDPE33. It is obvious that the general results agree with PEVA18, even if the data are less accurate. Independent of the temperature, we find three critical strains, located at $\epsilon_H \approx 0.03$ (A), $\epsilon_H \approx 0.13$ (B) and $\epsilon_H \approx 0.6$ (C).

The HDPE sample has much smaller recoverable strain components than the copolymer, which makes it difficult to detect the characteristic points in a step-cycle run. Here, we employed the free shrinkage experiment and determined the strain $\epsilon_{H,r}$ remaining after a sudden unloading. It comes close to the base part in the step-cycle test, that is, $\epsilon_{H,r} \approx \epsilon_{H,b}$. Figure 8 shows $\epsilon_{H,r}$ plotted as a function of the total strain. Although heating

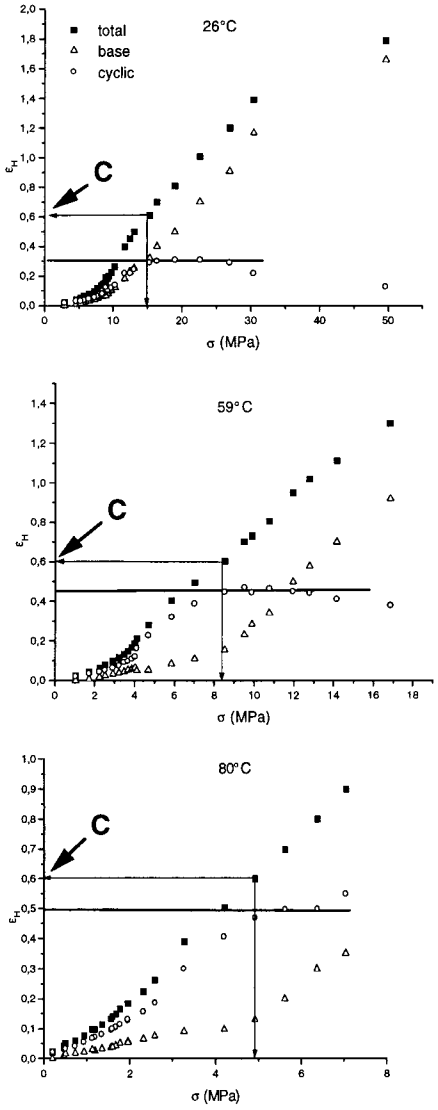

Figure 6. Total strain, base part, and cyclic component as a function of imposed stress, derived for LDPE33 from step-cycle tests under variation of the temperature.

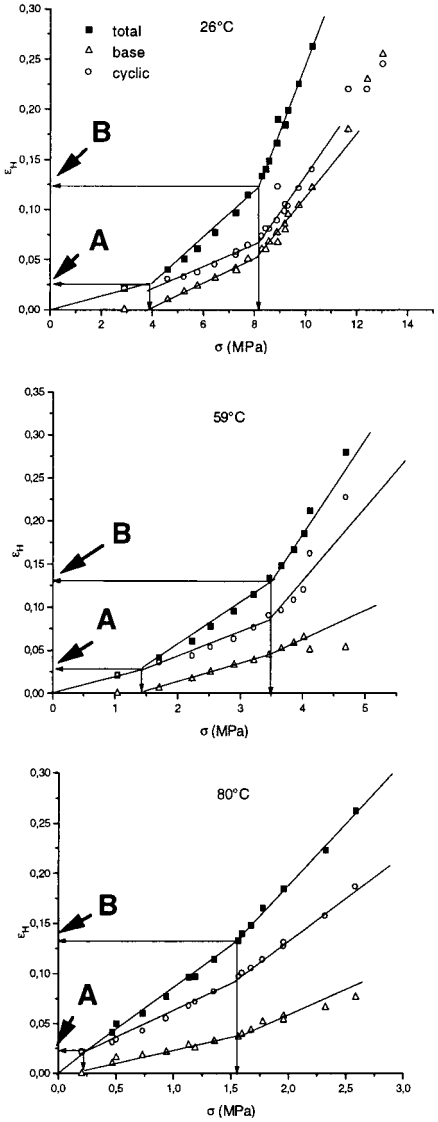

Figure 7. LDPE33 at different temperatures: partitioning of the total strain into the cyclic and the base component for small strain values (enlarged view from Figure 6).

results in higher retracting forces, which could in principle reduce the remaining strain, this is not observed. Permanent deformations arise from $\epsilon_H \simeq 0.1$, in the range of the points A and B, and at C a break is seen, located for all temperatures at $\epsilon_H \approx 0.6$.

Finally, when the free shrinkage experiment is combined with heating to the melting point, one can detect the fourth transition point, D, where disentangling leads to a true plastic deformation. Here, different from the critical strains A, B, and C, we do see a temperature effect. One observes a tendency to a lowering of the related strain with increasing temperature, down to the location of point C.

The figures in this section give an impression of the accuracy of the data. As always in deformation tests, this accuracy is not too high, and one finds corresponding variations when repeating the experiments taking another sample. Despite this variation, the existence of critical points, where the yielding process changes, shows up clearly, and their locations are quite well determined.

3.3. Effect of Strain Rate on Deformation Behavior. To study the influence of the deformation rate on the mechanical behavior, video-controlled tensile tests at several constant strain rates were performed. Figure 9 shows the true stress−strain curves for both materials, obtained for constant local strain rates in the range of $\epsilon_H = 10^{-2}$ to 10^{-4} s^{-1}. For the HDPE sample, there is a pronounced effect, as decreasing the strain rate remarkably lowers the stresses at all strains. For the copolymer, the difference in stress for the various strain rates is smaller although still observable. As pointed out previously (compare Figure 5 in Hiss et al.[1]), for HDPE the stress−strain rate dependence as observed in the plateau after the yield point is indicative of an Eyring process. Now, we note in addition that, although yield stresses increase with rate, the yield strains, as given by the location with the largest change in the differential compliance, do not change. They are always in the range $\epsilon_H \approx 0.12 \pm 0.02$.

Figure 10 shows cyclic and base strain components determined by the step-cycle test in the case of PEVA18, carried out for different strain rates. One finds that the total strain ϵ_H at point C does not change, while the related stress increases with strain rate. Figure 11 depicts analogous data for LDPE33, leading to the same result.

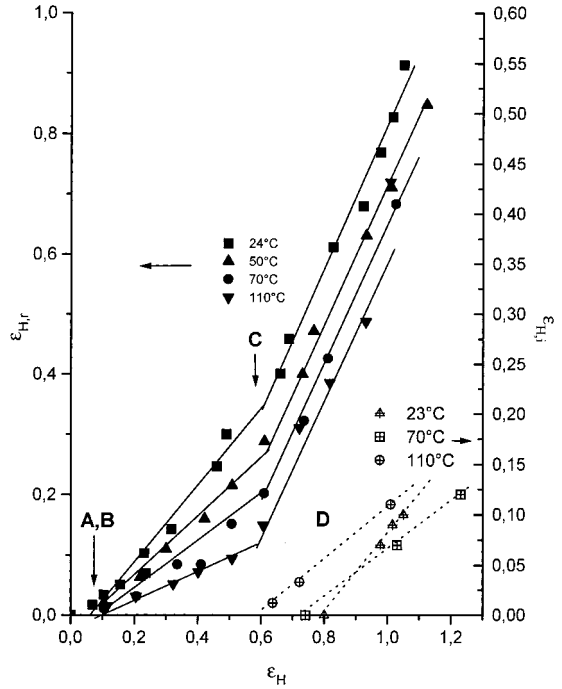

Figure 8. Persisting strain after sudden unloading in a free shrinkage experiment at several temperatures ($\epsilon_{H,r}$) and after heating the sample up to its melting point ($\epsilon_{H,i}$) for HDPE as a function of the total deformation.

Figure 12 shows for HDPE the results of free shrinkage experiments carried out after deformations with various strain rates, plotting the remaining part $\epsilon_{H,r}$ as a function of total strain. Data points for all strain rates fall onto one line, beginning with the activation of the slip processes at points A and B and showing a break at $\epsilon_H = 0.6$, that is, at point C, associated with the beginning of fibrillation. Obviously, not only does the critical total strain not change with strain rate, but the partitioning into cyclic and base component is also independent. For the truly plastic deformation, as given by the irreversible part of the strain remaining even after heating, one finds for HDPE no strain rate dependence.

4. Discussion

The observed effects of temperature and strain rate at the stresses during a stretching show the expected tendencies: decreasing strain rate and increasing temperature generally result in a lowering of the stress needed to reach a given strain. Although for PEVA18 and LDPE33, heating also results in a lower content of crystalline material, in the case of HDPE, crystallinity is not much changed in the given temperature range. We therefore must conclude that the stresses, in particular those at the critical points B and C, show, in addition to the known effect of the crystallinity, an explicit dependence on temperature.

In a global view, the yielding behavior of polyethylene may be addressed as the deformation of the network set up by the entanglements under conditions of a high internal viscosity. Variation of the temperature, the strain rate, and, caused by the partial melting, the crystallinity changes only the internal friction component. Physically, this friction comes from inter- and intralamellar shear processes. It increases with the volume fraction of the sheared crystalline material, because the area of the slipping surfaces is increased,

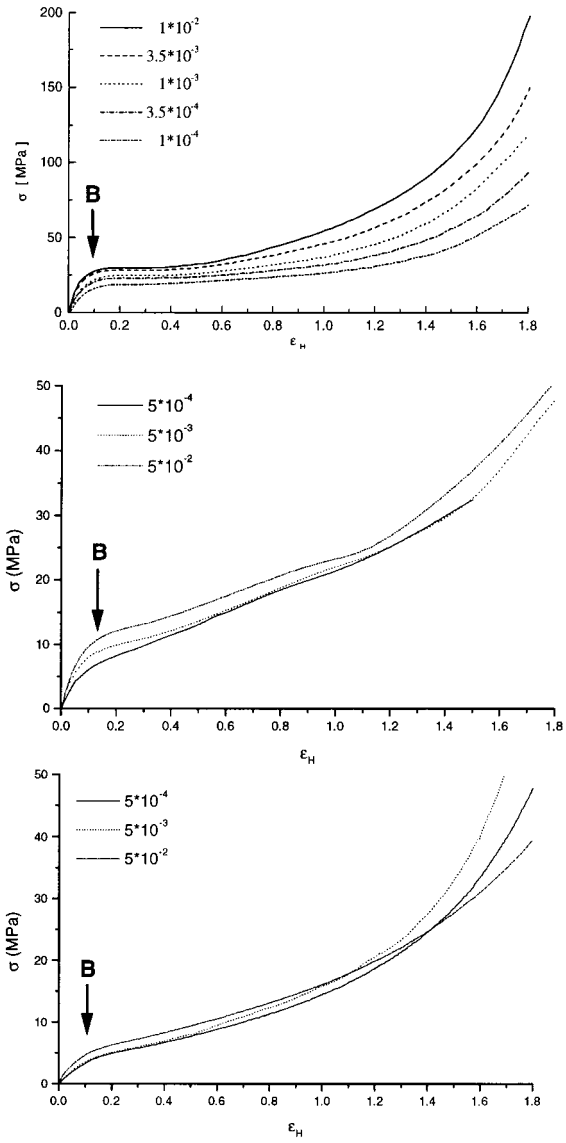

Figure 9. Strain rate dependence of true stress−strain curves at room temperature for HDPE (*top*), LDPE33 (*center*), and PEVA18 (*bottom*). Strain rate unit in the legend is s^{-1}.

and with strain rate as a consequence of a higher local deformation speed. Heating facilitates rearranging of the texture, as the viscosity of the amorphous intercrystalline layers decreases. For the copolymer, it additionally results in a lower volume content of crystallites, which further supports the stress lowering effect.

The shear processes induced by the stretching change the amorphous−crystalline texture in stepwise fashion; first locally, then by rearrangement of the whole lamellar structure, followed by breaking up the lamellae and forming fibrils, and last by disentanglement, which finally leads to fracture of the sample. Material behavior changes show up clearly at the transition points A, B, C, and D under variation of temperature and strain rate changes show up directly in the stress−strain curve as an increase in the differential compliance at the yield point (Figures 3 and 9), in the step-cycle experiment as changes in the (linear) dependence of the cyclic strain component and the base part on the total strain (Figures 4, 5, 6, 7, 10 and 11), and in the first occurrence of a truly plastic deformation persisting after a heating (Figures 8 and 12).

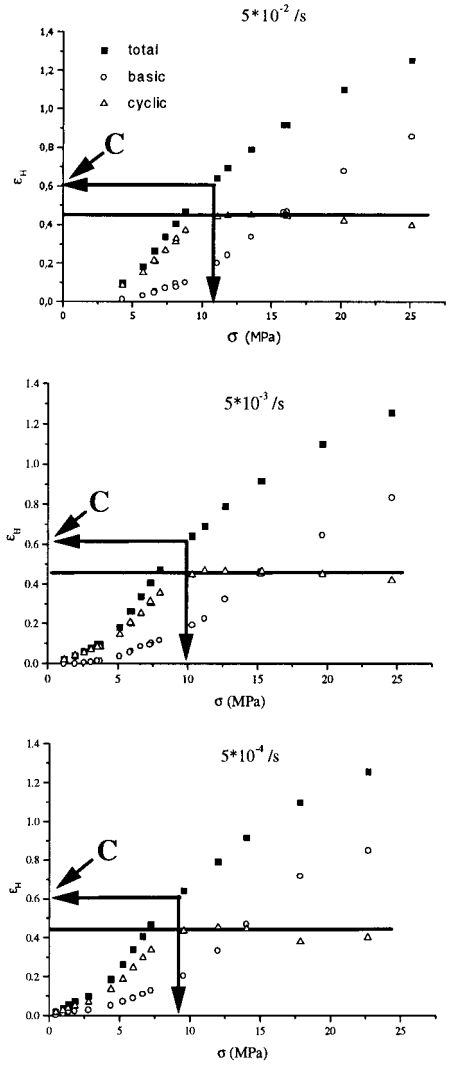

Figure 10. Total strain, base part, and cyclic strain component as a function of imposed stress, derived from step-cycle tests for PEVA18 under variation of the strain rate.

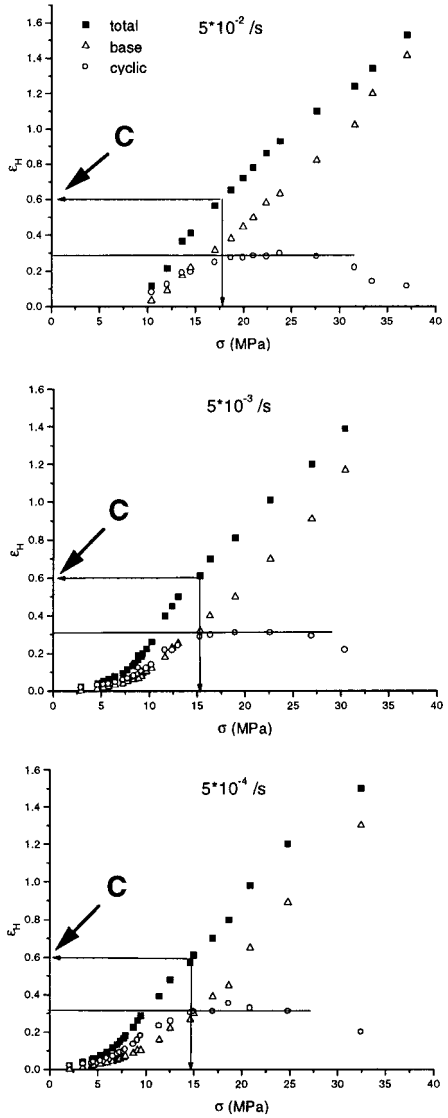

Figure 11. Total strain, base part, and cyclic strain component as a function of imposed stress, derived from step-cycle tests for LDPE33 under variation of the strain rate.

In contrast to the stresses at the transition points A, B, and C, which greatly vary, the critical strains at these points are not affected by changes in the temperature and the strain rate. This is an important finding. It complements and fits with the previously observed independence on the crystallinity. As long as the underlying entanglement network is not destroyed, activation of the different deformation steps during stretching is only strain dependent. Neither sample crystallinity nor mechanical or thermal history change the critical strain values at the transition points, which means that in order to reach a given strain the sample texture has to change in a well-defined manner. As discussed previously, this is only possible if there were at least five slip systems to enable the amorphous−crystalline system to react to the imposed stress. At each critical strain, the deformation limit that can be realized through a certain shear process is reached, so the next step in the sequence of deformation processes has to start.

As the only exception, opposite to points A, B, and C, at point D heating shows an effect: Figure 8 depicts the truly irreversible strain $\epsilon_{H,i}$ which persists in the free shrinkage experiment even after heating to the melting point as a function of total deformation for a range of temperatures. One can see a tendency that, at higher deformation temperatures, true plastic deformation sets in at lower strains. The behavior is conceivable. The disentangling process, which is related to this characteristic strain, becomes easier at high temperatures and thus may set in already at a lower strain because the mobility of the chains increased.

In comparison, as shown by the strain rate independence of the strain at point D, the deformation time does not play a role in the onset of this process for the strain rates used here. As we see, neither the partitioning of the total strain into an elastic and a remaining component nor the irreversible part is affected by the alteration of the strain rate. This means that inter- and intralamellar slips as well as fragmentation and disentangling have to take place fast enough, so that no retardation occurs.

Decisive for the finding of the critical strain laws is the determination of true stress−strain curves for constant strain rates, as obtained by employing the video-control. The normal engineering stretching curves registered with constant cross-head speed cannot provide these results. Indeed, load-extension curves measured for necking samples such as HDPE and LDPE change their shape with temperature, as shown in

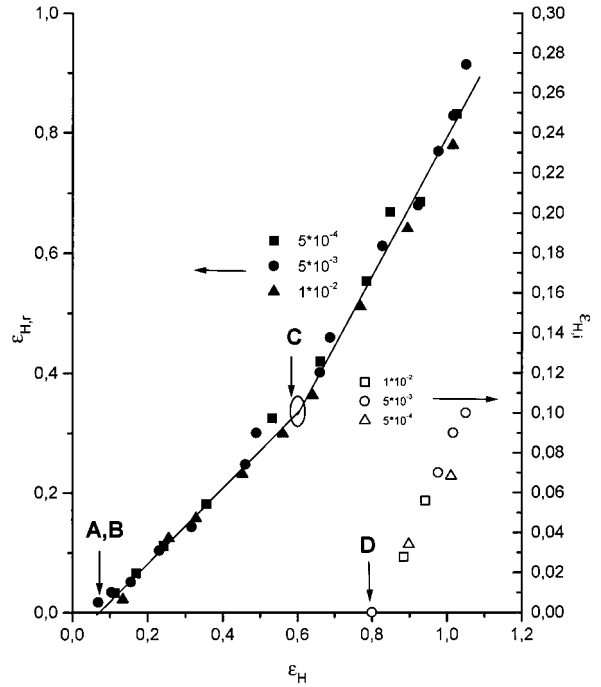

Figure 12. Persisting strain after sudden unloading in a free shrinkage experiment ($\epsilon_{H,r}$) and after heating the sample up to its melting point ($\epsilon_{H,i}$) as a function of the total deformation, observed for different strain rates for HDPE.

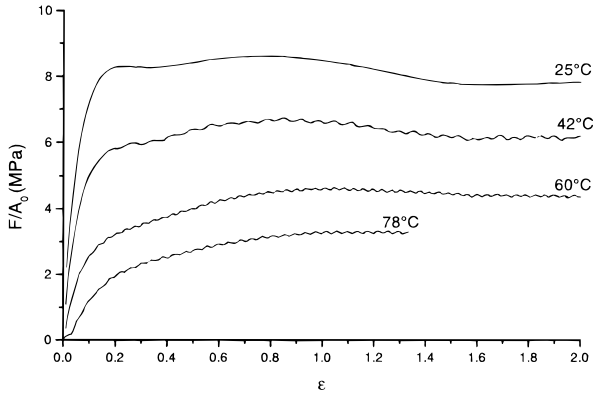

Figure 13. LDPE33: engineering load−extension curves measured at the indicated temperatures.

Figure 13 for the case of LDPE33. There is no longer the systematic variation of the true stress−strain curves showing up in Figure 3. In particular, the engineering yield point, as given by the load maximum, may well shift in strain with temperature, as is reported, for example, in a recent paper on HDPE of Brooks et al.[6] In fact, in contrast to point B, which can be associated with the collective onset of slip processes, the engineering yield point, although of technical importance, has no simple physical background. Its location depends on the shape of the true stress−strain curve in a larger range above B, the change of stresses with the strain rate, and the variations with time of the acting force. Hence, it is not surprising that the critical strain laws, indicated by our experiments, did not show up in previous studies.

5. Conclusion

In our study of the deformation behavior of polyethylenes and related copolymers, we focused here on the temperature and strain rate dependence of the four transition points, where the yielding and the elastic recovery properties of the samples change. As explained previously, each point is related to the onset of a microscopic deformation process, namely, isolated inter- and intralamellar slips (point A), a transition to a collective shear (point B), fragmentation of the lamellar structure and formation of fibrils (point C), and disentangling of the entanglement network (point D). Although the stresses at points A, B, and C decrease upon heating or lowering of the strain rate, the characteristic strains remain constant. This means that the activation of each process is strain controlled and has its origin in a limited strain that can be realized by the deformation processes begun previously. At point D, where true plastic deformation sets in, one finds a temperature-dependent critical strain as a consequence of the higher mobility of the chains, which facilitates disentangling, but still no strain rate dependence. The well-defined reaction of the semicrystalline polymer system, which is dependent only on the imposed strain, supports the recently suggested picture of granular lamellae, for such a blocklike substructure would be able to rearrange in the way needed.

Acknowledgment. Support of this work by the Deutsche Forschungsgemeinschaft (Sonderforschungsbereich 428 and Graduiertenkolleg Strukturbildung in Makromolekularen Systemen) is gratefully acknowledged. Thanks are also due to the Fonds der Chemischen Industrie for financial help.

References and Notes

(1) Hiss, R.; Hobeika, S.; Lynn, C.; Strobl, G. *Macromolecules* **1999**, *32*, 4390.
(2) Hugel, T.; Strobl, G.; Thomann, R. *Acta Polym.* **1999**, *50*, 214.
(3) Heck, B.; Hugel, T.; Iijima, M.; Sadiku, E.; Strobl, G. *New J. Phys.* **1999**, *1*, 17.
(4) Strobl, G. *The Physics of Polymers*; Springer: New York, 1997.
(5) G'Sell, C.; Hiver, J. M.; Dahoun, A.; Souahi, A. *J. Mater. Sci.* **1992**, *27*, 5031.
(6) Brooks, N. W. J.; Duckett, R. A.; Ward, I. M. *Polymer* **1999**, *40*, 7367.

MA9910484